Chemical Science

Accepted Manuscript

This article can be cited before page numbers have been issued, to do this please use: X. Pan, Y. Zhao, T. Cheng, A. Zheng, A. Ge, L. Zang, K. Xu and B. Tang, *Chem. Sci.*, 2019, DOI: 10.1039/C9SC02020A.

ROYAL SOCIETY OF CHEMISTRY

rsc.li/chemical-science

ROYAL SOCIETY OF CHEMISTRY View Article Online
DOI: 10.1039/C9SC02020A

Journal Name

ARTICLE

Received 00th January 20xx,
Accepted 00th January 20xx

DOI: 10.1039/x0xx00000x

www.rsc.org/

Monitoring NAD(P)H by an ultrasensitive fluorescent probe to reveal reductive stress induced by natural antioxidants in HepG2 cells under hypoxia

Xiaohong Pan[a,b], Yuehui Zhao[a], Tingting Cheng[b], Aishan Zheng[a], Anbin Ge[b], Lixin Zang[a], Kehua Xu *[a], and Bo Tang *[a]

Reductive stress, the opposite of oxidative stress, represents a disorder in the redox balance state that is harmful to biological systems. For decades, the role of oxidative stress in tumor therapy has been the focus of attention, while the effects of reductive stress have been rarely studied. Here, we reported the anti-cancer effects of reductive stress induced by three natural antioxidants (resveratrol, curcumin and celastrol). Considering that the solid tumor microenvironment suffers from hypoxia, we performed the cell experiments under hypoxic conditions. In order to observe the reductive stress, we first developed an ultrasensitive fluorescent probe (TCF-MQ) for specifically imaging NAD(P)H which is a marker of reductive stress. TCF-MQ responded to NAD(P)H rapidly and exhibited high sensitivity with a detection limit of 6 nM. With the help of TCF-MQ, we found that pharmacological doses of three natural antioxidants treatment of HepG2 cells under hypoxic conditions, high levels of NAD(P)H were produced before cell death. The excess NAD(P)H resulted in reductive stress instead of oxidative stress. In contrast, under normoxic conditions, there was no reductive stress involved in the process of cell death induced by three natural antioxidants. Therefore, we hypothesize that the mechanism of cancer cell death induced by natural antioxidants under hypoxia should be attributed to the reductive stress.

Introduction

Natural antioxidant, such as resveratrol, curcumin or celastrol, is a self-protective substance produced by organisms to resist poor environment and reactive oxygen species (ROS). It mainly exists in fruits, vegetables and medicinal plants. Due to the antioxidant and free radical scavenging effects, natural antioxidant is traditionally used as food protection and disease prevention. Recently, several natural antioxidants have been reported to possess anti-tumor effects[1-3], but the mechanisms underlying their anticancer functions are debated. Most studies suggest that some natural antioxidants can stimulate the production of ROS to cause oxidative stress, which leads to cell apoptosis[4-6]. However, these results are contradictory to their antioxidant effects. We found that there is a common feature in the above studies, that is, the tumor cells used in the experiments are all cultured under normoxic conditions (20% O_2), there is abundant oxygen around the cells, which provides conditions for the production of reactive oxygen species[7]. But this condition is obviously contrary to the hypoxic microenvironment of solid tumors[8,9]. Hypoxia is a common feature in solid tumors. In hepatocellular carcinoma (HCC), the O_2 values in most areas is in the range of 0-10 mmHg (0-1.32%)[10]. Therefore, in this study, we revealed a new anti-cancer mechanism of three natural antioxidants (resveratrol, curcumin and celastrol) under the simulated tumor hypoxic conditions.

The redox balance in the body is the fundamental to sustain life. Once redox imbalanced, cell damage and apoptosis are inevitable[11-13]. For decades, studies on the anti-tumor effects of natural antioxidants have been focused on the oxidative stress. However, reductive stress, another way of redox imbalance, is rarely noticed. Similar to oxidative stress, reductive stress also represents a disturbance in the redox state which can cause body damage and lead to cell death[14-16]. Recently, reductive stress is defined as an excessive amount of reducing equivalents, and excess NAD(P)H and/or GSH is considered a marker of reductive stress[14,17,18].

NAD(P)H, the general term of the nicotinamide adenine dinucleotide (NAD) derivatives NADH and NADPH[19], is universal electron carrier in cellular processes. The NAD(P)H and $NAD(P)^+$ undergo reversible oxidation-reduction in many biological reactions[20], and the level of NAD(P)H is tightly

[a] College of Chemistry, Chemical Engineering and Materials Science, Key Laboratory of Molecular and Nano Probes, Ministry of Education, Collaborative Innovation Center of Functionalized Probes for Chemical Imaging in Universities of Shandong, Shandong Normal University, Jinan 250014, P. R. China.
[b] Department of Pharmaceutical Sciences, Binzhou Medical University, Yantai 264003, P. R. China.
E-mail: tangb@sdnu.edu.cn; xukehua@sdnu.edu.cn.
†Electronic Supplementary Information (ESI) available:

DOI: 10.1039/C9SC02020A

linked to the redox environment in cells. Insufficient NAD(P)H induces oxidative stress due to increased ROS production, while excessive NAD(P)H leads to reductive stress because it cannot be properly oxidized[20]. Besides, NAD(P)H is a highly reducible dynamic molecule with very high reactivity and instability that cannot be easily detected in cells and animal models. Therefore, an ultrasensitive and rapid method to selectively determine NAD(P)H in vivo must be developed to investigate the reductive stress.

Fluorescent probe offers a powerful tool for direct visualization of biomolecules in vivo with high sensitivity and short response times[21,22]. To date, detection methods for reductive stress have been reported[23-25], and in particular, several small-molecule fluorescent probes for detecting NAD(P)H have been developed[26-31]. Louie et al. synthesized a NADH-sensitive multimodal magnetic-resonance/optical-imaging contrast agent and successfully applied it in cells[27]. Komatsu reported an ubiquinone-rhodol-derived fluorescent probe for imaging intracellular NAD(P)H[29]. Recently, Chang et al. developed a boronic acid-containing fluorescent probe for NADH based on resazurin, which shows dramatically improved sensitivity (detection limit: 0.084 μM) by introducing boronic acid to bind with NADH[31]. In addition, our group previously developed a near-infrared small-molecule fluorescent probe (DCI-MQ) based on dicyanoisophorone for monitoring of NAD(P)H in cells[32]. This probe was successfully used to selectively detect the endogenous NAD(P)H in cells with a detection limit of 12 nM. Although the above methods for detecting NAD(P)H are suitable for cell use, these methods are not suitable for monitoring the reductive stress due to their lower sensitivity.

Here, we designed and synthesized an ultrasensitive small-molecule fluorescent probe (TCF-MQ) for better detecting NAD(P)H. TCF-MQ chose a more electron-absorbing tricyanofuran as the chromophore which enables the probe has good sensitivity for NAD(P)H with the limit of detection (LOD) was 6 nM. This probe was successfully used to distinguish the different levels of NAD(P)H in HepG2 cells under normoxic and hypoxic conditions. Furthermore, with the help of TCF-MQ, we found that high levels of NAD(P)H were produced before cell death after pharmacological doses of natural antioxidants (resveratrol, curcumin and celastrol) treatment of HepG2 cells under hypoxic conditions. The excess NAD(P)H resulted in reductive stress which might induce the cell death.

Results and discussion

Design and Synthesis of TCF-MQ.

2-Dicyanomethylene-3-cyano-4,5,5-trimethyl-2,5-dihydrofuran (TCF) as an strong electron-withdrawing group has been widely used in non-linear optical materials[33,34]. For TCF-based fluorophores typically have a donor-π-acceptor (D-π-A) structure with long emission wavelengths, many fluorescent probes have been developed[35]. Here, we designed and synthesized a TCF-based fluorescent probe (TCF-MQ) for the detection of NAD(P)H (Scheme 1). TCF-MQ and all intermediate structures were fully characterized by ^{1}H NMR, ^{13}C NMR, and HRMS (see Experimental Section and Supporting Information).

Scheme 1. Synthesis of TCF-MQ

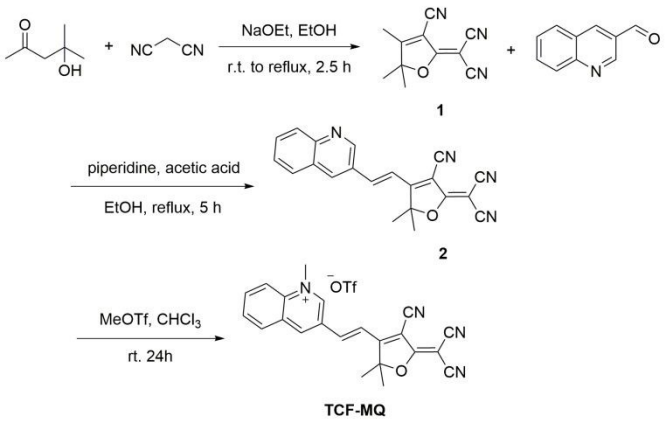

The proposed recognition mechanism of TCF-MQ toward NAD(P)H is shown in Scheme 2. The active hydrogen atom of NAD(P)H was added to the quinolinium moiety of the probe to form the adduct. To verify the sensing mechanism of TCF-MQ for NADH, the probe TCF-MQ and the product of TCF-MQ with NADH were analyzed by ESI-HRMS and ^{1}H NMR spectroscopy. Once the reaction of TCF-MQ with NADH was completed, a mass peak at 353.1477 (*m/z* calcd = 353.1396) belonging to the reaction product was observed (Scheme 2, Fig. S1). From the ^{1}H NMR analysis, after the reaction of TCF-MQ with NADH, the N-CH_3 protons of TCF-MQ upfield shifted from 4.68 to 3.54 ppm, and a new singlet at 3.87 ppm emerged (Fig. S2). These data confirmed our proposed recognition mechanism.

Scheme 2. TCF-MQ for Fluorescent Detection of NAD(P)H

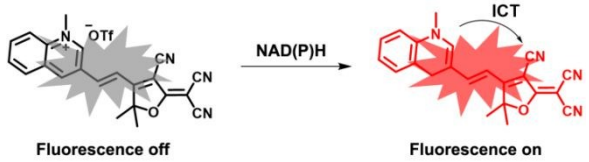

Fluorescent performance analysis of TCF-MQ.

The spectral properties of the probe with or without NADH were measured in PBS buffer solution (0.5 % DMSO, 10 mM PBS, pH = 7.4). As shown in Figure 1a, the probe displayed a weaker fluorescence peak at 604 nm (λ_{ex} = 576 nm). As expected, after the reaction of the probe with NADH, a significant fluorescence enhancement at 610 nm (λ_{ex} = 582 nm) was observed (Quantum Yield = 0.064). Meanwhile, the fluorescence intensity at 610 nm was enhanced gradually and reached a plateau within 25 min (Fig. 1b). The effect of pH on the fluorescent detection of NADH with TCF-MQ was also investigated, which indicated that TCF-MQ responded to NADH well under physiological conditions (at 37 °C and pH =7.4) (Fig. S3).

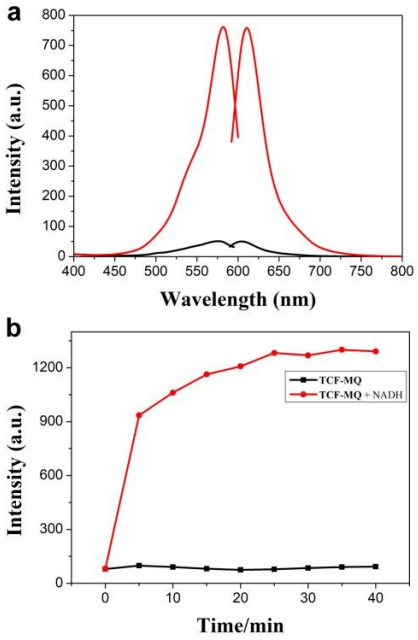

Figure 1. (a) Excitation and emission spectra of TCF-MQ (black) and the product of TCF-MQ with NADH (red). (b) Time-dependent fluorescence changes of TCF-MQ (10 μM) upon addition of NADH (50 μM).

Next, we investigated the sensitivity of the probe to NADH. The spectra of the solution of TCF-MQ treated with different concentrations of NADH (0 to 50 μM) were recorded. Upon treatment with NADH, the fluorescence intensities at 610 nm gradually increased with increasing concentrations of NADH (Fig. S4), and there was a good linearity between the fluorescence intensities and NADH concentrations in the range of 0-3 μM (Fig. 2a). The regression equation is F = 83.22 + 238.42 [NADH], with a linear coefficient of 0.9819. The limit of detection (LOD) was calculated to be as low as 6 nM on the basis of S/N=3, which indicates that TCF-MQ has excellent sensitivity to NADH and is more suitable for detecting NADH in living systems than DCI-MQ (LOD=12 nM)[26].

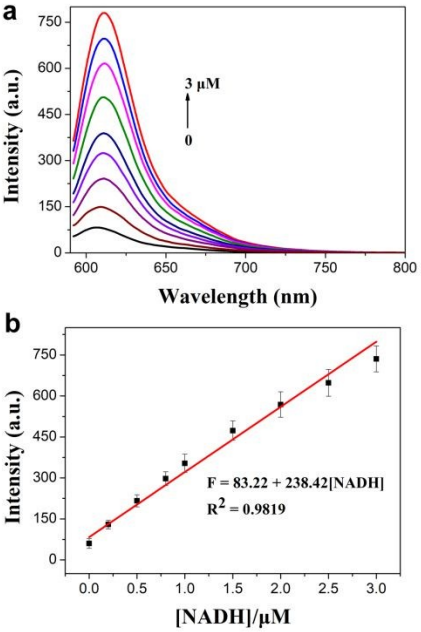

Figure 2. (a) Fluorescence intensities changes of TCF-MQ (10 μM) upon addition of different concentrations of NADH (0−3 μM) in PBS (10 mM, pH 7.4, 0.5% DMSO as acosolvent) at 37 °C for 30 min. (b) A linear correlation between emission intensities and concentrations of NADH. λ_{ex} = 582 nm, λ_{em} = 610 nm, slit width: 5 nm /5 nm.

Selective recognition of NAD(P)H by TCF-MQ.

To illustrate the good selectivity of TCF-MQ toward NAD(P)H, a series of biologically relevant species including inorganic salts, amino acids and reducing agents were evaluated. As shown in Figure 3, compared with NADPH and NADH, inorganic salts (K^+, Na^+, Ca^{2+}, Mg^{2+}, Zn^{2+}, Fe^{3+}, Fe^{2+}), amino acids (glycine, lysine, methionine, serine, cysteine, homocysteine), reducing agents (glutathione, Vitamin C, dithiothreitol, H_2S_2, SO_3^{2-}), NAD^+, $NADP^+$ and $FADH_2$ did not cause obvious changes of the fluorescence intensity indicating not interfere with the detection of NAD(P)H. In addition, the reactivity of TCF-MQ toward ROS was also tested. The results showed that biologically relevant ROS, including $O_2^{\bullet-}$, H_2O_2, NaClO, *t*-BuOOH and NO, did not trigger any fluorescence changes in the probe solution (Fig. S5). These results demonstrate that TCF-MQ can be employed for specific recognition of NAD(P)H with high selectivity.

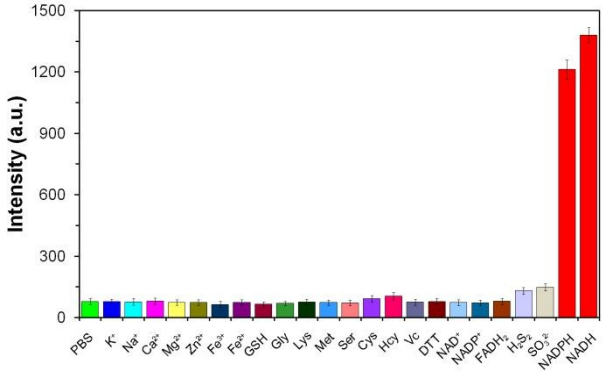

Figure 3. Fluorescence responses of probe TCF-MQ (10 μM) for various analytes: 1 mM of (K^+, Na^+, Ca^{2+}, Mg^{2+}, Zn^{2+}, Fe^{3+}, Fe^{2+}, GSH, Gly, Lys, Met, Ser); 100 μM of (Cys, Hcy, VC, DTT); 5 μM of (H_2S_2, SO_3^{2-}); and 50 μM of (NAD^+, $NADP^+$, $FADH_2$, NADPH, NADH).

Bioimaging of NAD(P)H in living cells.

After confirming the high sensitivity and selectivity of TCF-MQ for NAD(P)H, we explored its applications to image endogenous NAD(P)H in living cells. Before applied to cell imaging, we first tested the cytotoxicity of this probe by a MTT assay. The result showed that the TCF-MQ probe exhibited negligible cytotoxicity when HepG2 cells were treated with 0-50 μM probe for 18 h (Fig. S6). The resistance to photobleaching experiments showed that no obvious fluorescence decrease was observed when cells were exposured to the laser radiation for 600s (Fig. S7), suggesting the probe is stable and can be used as a viable probe in living cells.

Previous studies have shown that hypoxia can enhance NAD(P)H levels [36,37]. Here, we investigated the imaging ability

of TCF-MQ for NAD(P)H in HepG2 cells under hypoxia (1% O_2) and normoxia (20% O_2), respectively. HepG2 cells were cultured under hypoxic or normoxic conditions for 12 h, and then incubated with 10 μM TCF-MQ for 5-25 min. As shown in Figure 4, the fluorescence of TCF-MQ reached the brightest within 15 min, and the fluorescence intensity under hypoxia was higher than that under normoxia, indicating that more NAD(P)H was generated in cells under hypoxia. This result indicates that the probe can be used to monitor the levels of NAD(P)H in living cells.

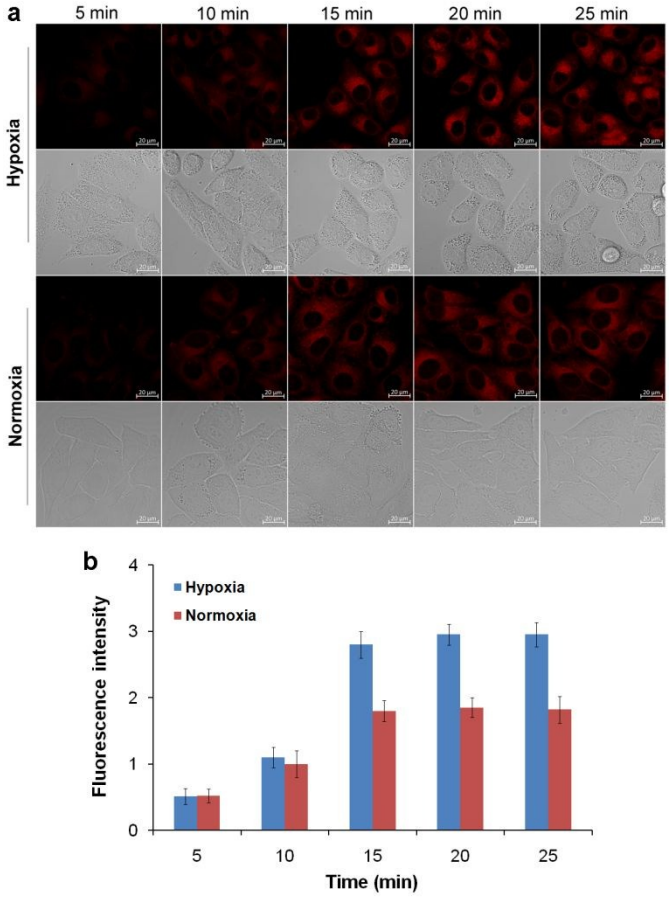

Figure 4. Fluorescence imaging of NAD(P)H in living cells. HepG2 cells were cultured under hypoxic (1% O_2) or normoxic (20% O_2) conditions for 12 h, and then incubated with 10 μM of the TCF-MQ probe for 5-25 min. (a) The fluorescence images were obtained using confocal microscopy. (b) The fluorescence intensity was quantified based on the results of the relative fluorescence intensity of per cell in the scanned area. The scale bar in all fluorescence images of cells is 20 μm.

Revealing reductive stress induced by natural antioxidants.

Next, we used the TCF-MQ probe to observe the NAD(P)H levels in the process of liver cancer cell death induced by natural antioxidants (resveratrol, curcumin and celastrol). HepG2 cells were exposed to different concentrations of resveratrol, curcumin and celastrol for different time under hypoxic and normoxic conditions, respectively. After treatment, the cells were loaded with 10 μM TCF-MQ for 20 min, then, the fluorescence was detected by confocal microscopy. Under hypoxic conditions, the HepG2 cells treated with 0-10 μg/mL resveratrol for 6 h had a concentration-dependent increase in fluorescence. However, when the resveratrol concentration reached 20 μg/mL, the fluorescence intensity decreased due to the cell was going to die (Fig. 5a, d and g). Additionally, after the HepG2 cells were treated with 10 μg/mL resveratrol for 0-9 h, the fluorescence intensity was also enhanced in a time-dependent manner (Fig. S8). In contrast, under normoxic conditions, after the HepG2 cells were exposed to 0-20 μg/mL resveratrol for 6 h or 10 μg/mL resveratrol for 0-9 h, the cells exhibited much lower fluorescence compared with that under the hypoxic conditions, and there was no enhancement of fluorescence in the process of cell death (Fig. 5a, d and g, Fig. S8). Curcumin and celastrol showed similar results to resveratrol. When HepG2 cells were treated with curcumin or celastrol under hypoxic conditions, the fluorescence intensity of NAD(P)H was increased in a concentration- and time-dependent manner, but decreased with cell death (Fig. 5b-i). However, under normoxic conditions, only intracellular background fluorescence of TCF-MQ was observed during cell death induced by curcumin and celastrol (Fig. S9 and 10). These results indicate that reductive stress is involved in the process of HepG2 cell death induced by resveratrol, curcumin and celastrol, and the cell death may be attributed to the reductive stress.

Because previous studies have shown that natural antioxidants (resveratrol, curcumin and celastrol) can stimulate the production of ROS in tumor cells cultured in vitro[4-6], we assessed whether oxidative stress was induced as HepG2 cells were treated with the above three natural antioxidants under hypoxic conditions. In this experiment, a previously described H_2O_2 probe was employed[38]. HepG2 cells were exposed to resveratrol (10 μg/mL), curcumin (10 μg/mL) and celastrol (2 μg/mL) for 0-9 h under hypoxic conditions, respectively. Then, the cells were incubated with the H_2O_2 probe for 15 min. As a result, there were no obvious increase in H_2O_2 levels in the three antioxidant treatment groups compared with the control group (Fig. S11-13). These results indicate that the three antioxidants do not cause oxidative stress under hypoxic conditions.

To further confirm the reductive stress induced by natural antioxidants in HepG2 cells under hypoxic conditions, we conducted a similar experiment *in vivo*. Tumor bearing mice were treated with different concentrations of resveratrol, curcumin and celastrol via subcutaneous injection at the tumor site for 10 days. After treatment, the mice received a subcutaneous administration of the TCF-MQ probe (10 μM) into the tumor and incubated for 30 min. Then, the fluorescence images were obtained using an *in vivo* imaging system. The fluorescence signal of the probe was obviously increased in a dose-dependent manner in the resveratrol treatment groups (Fig. 6a and d). Similar to the resveratrol results, the fluorescence intensity of the probe was also enhanced in the curcumin and celastrol treatment groups (Fig. 6b, c, e and f), indicating NAD(P)H levels were elevated during the three natural antioxidants treatment of liver cancer in mice. These findings support the *in vitro* results obtained using the HepG2 cells under hypoxia showing that reductive stress was induced by natural

View Article Online
DOI: 10.1039/C9SC02020A

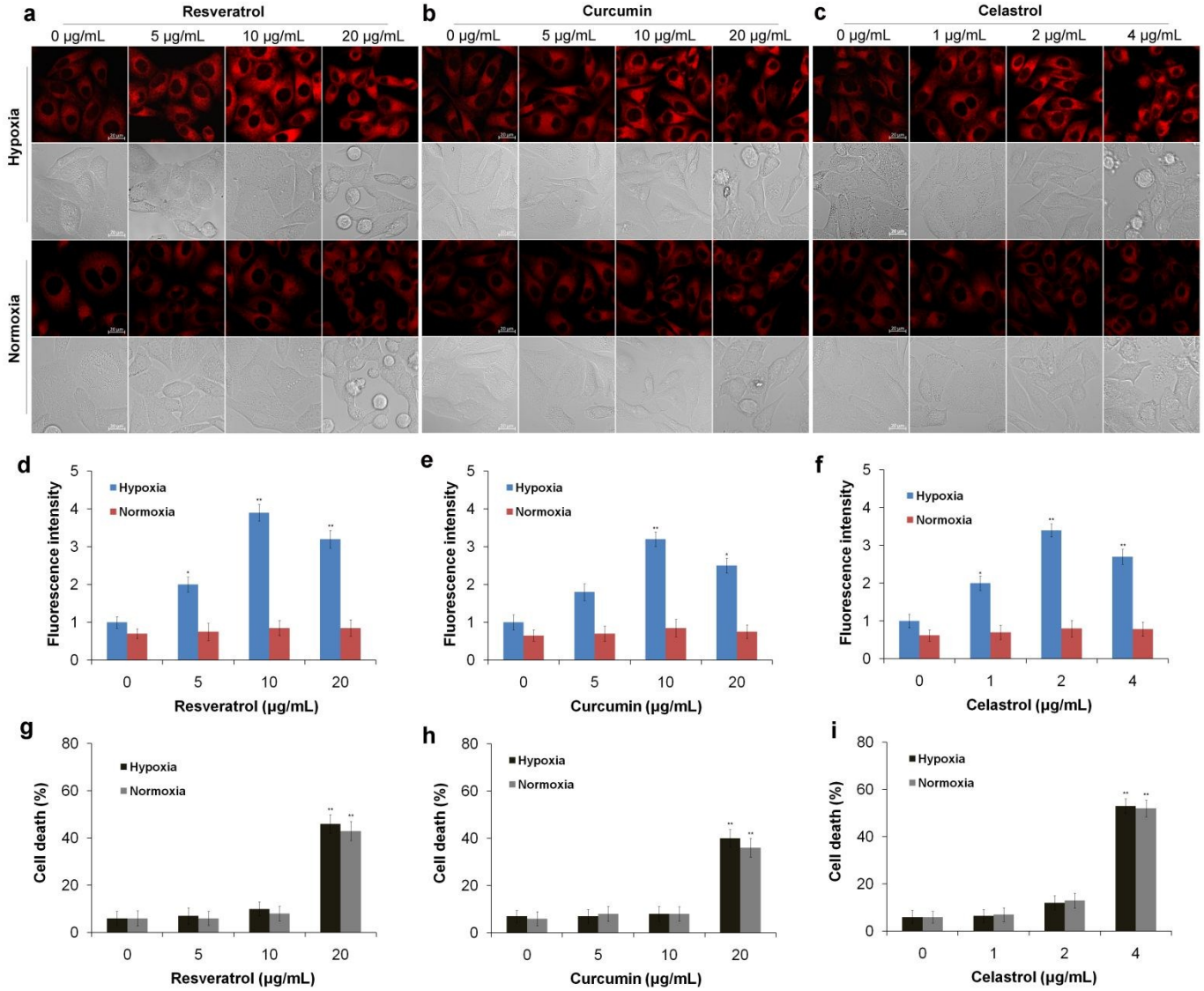

Figure 5. Detection of NAD(P)H levels induced by natural antioxidants in living cells. (a) HepG2 cells were exposed to 0-20 μg/mL resveratrol for 6 h under hypoxic conditions (1%O_2) and normoxic conditions (20%O_2), then the cells were incubated with 10 μM of the TCF-MQ probe for 20 min before the fluorescence images were obtained using confocal microscopy. (b) HepG2 cells were exposed to 0-20 μg/mL curcumin for 6 h under hypoxic conditions (1%O_2) and normoxic conditions (20%O_2), then the cells were treated using the method described in (a). (c) HepG2 cells were exposed to 0-4 μg/mL celastrol for 6 h under hypoxic conditions (1%O_2) and normoxic conditions (20%O_2), then the cells were treated using the method described in (a). (d-f) The fluorescence intensity of Figure a-c were quantified based on the results of the relative fluorescence intensity of per cell in the scanned area. (g) HepG2 cells were exposed to 0-20 μg/mL resveratrol for 6 h under hypoxic conditions (1%O_2) and normoxic conditions (20%O_2), then the cells were collected and stained by trypan blue. (h) HepG2 cells were exposed to 0-20 μg/mL curcumin for 6 h under hypoxic conditions (1%O_2) and normoxic conditions (20%O_2), then the cells were collected and stained by trypan blue. (i) HepG2 cells were exposed to 0-4 μg/mL celastrol for 6 h under hypoxic conditions (1%O_2) and normoxic conditions (20%O_2), then the cells were collected and stained by trypan blue. (*p<0.05, **p<0.01, t test). The scale bar in all fluorescence images of cells is 20 μm.

antioxidants treatment. The tumor volume measurement experiments showed that resveratrol could significantly inhibit tumor growth in a dose- and time-dependent manner (Fig. 6g). Curcumin and celastrol could also suppress the tumor growth in mice (Fig. 6h and i), indicating the reductive stress induced by three natural antioxidants can inhibit the growth of liver cancer tumor.

Conclusions

In summary, we developed a novel small-molecule fluorescent probe, TCF-MQ, for monitoring of NAD(P)H and revealing the reductive stress. TCF-MQ can rapidly respond to NAD(P)H with good selectivity and exhibited very high

View Article Online
DOI: 10.1039/C9SC02020A

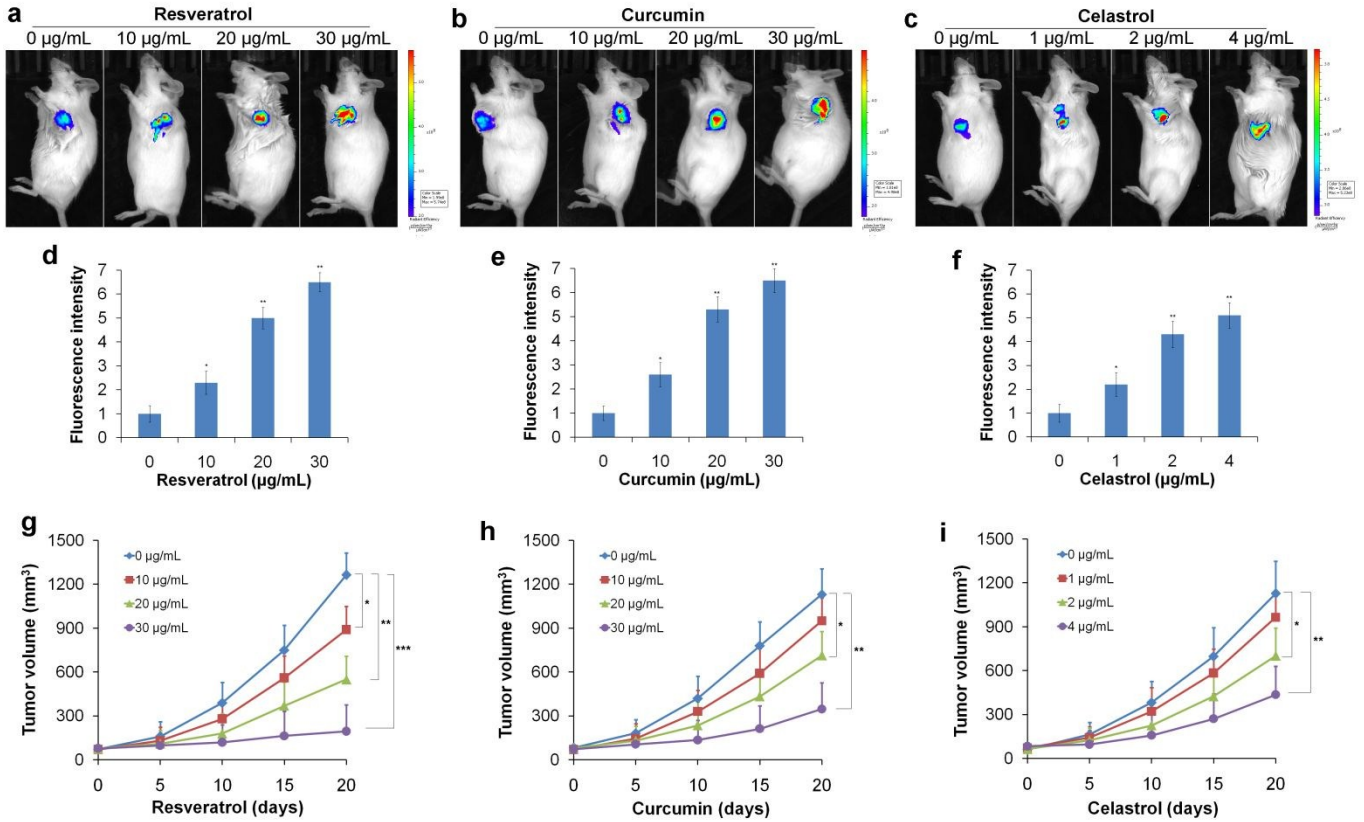

Figure 6. Detection of NAD(P)H levels induced by natural antioxidants *in vivo*. (a) Tumor-bearing mice were treated with 0-30μg/mL resveratrol for 10 days, and then, 10 μM TCF-MQ probe was subcutaneously injected into the tumor for 30 min before the fluorescence was analyzed using an *in vivo* imaging system. (b) Tumor-bearing mice were treated with 0-30μg/mL curcumin for 10 days, then the TCF-MQ probe was added using the method described in (a). (c) Tumor-bearing mice were treated with 0-4 μg/mL celastrol for 10 days, then the TCF-MQ probe was added using the method described in (a). (d) The quantitative fluorescence intensity for (a). (e) The quantitative fluorescence intensity for (b). (f) The quantitative fluorescence intensity for (c). (g) Tumor-bearing mice were treated with 0-30μg/mL resveratrol for different days, the tumor volumes were measured using digital calipers. (h) Tumor-bearing mice were treated with 0-30μg/mL curcumin for different days, the tumor volumes were measured using digital calipers. (i) Tumor-bearing mice were treated with 0-30μg/mL 0-4 μg/mL celastrol for different days, the tumor volumes were measured using digital calipers. (*p<0.05, **p<0.01, ***p<0.001, t test).

sensitivity to NAD(P)H with a low detection limit of 6 nM. The probe was successfully used to image endogenous NAD(P)H in living cells and to distinguish the different levels of NAD(P)H in HepG2 cells under normoxic conditions and hypoxic conditions. Moreover, with the help of TCF-MQ, we found that pharmacological doses of three natural antioxidants (resveratrol, curcumin and celastrol) treatment of HepG2 cells under hypoxic conditions, high levels of NAD(P)H were produced before cell death. The excess NAD(P)H resulted in reductive stress instead of oxidative stress. In contrast, under normoxic conditions, there were no obvious increase in NAD(P)H contents in the process of cell death induced by resveratrol, curcumin and celastrol. Thus, we speculate that natural antioxidants might induce tumor cell death via reductive stress under tumor hypoxic microenvironment, whereas under normoxic environment, natural antioxidants induced cell death through oxidative stress based on the previous reports[4-6]. The mechanism of reductive stress inducing tumor cell death under hypoxic conditions is undergoing further research. Our findings reveal a new anti-cancer mechanism of resveratrol, curcumin and celastrol and provide a new research area for natural antioxidants.

Experimental

Materials and methods**.** 3-Hydroxy-3-methyl-2-butanone, malononitrile, methyl trifluoromethanesulphonate and 3-quinolinecarboxaldehyde were purchased from Sun Chemical Technology (Shanghai, China). β-NADPH and β-NADH were obtained from Aladdin (Shanghai, China). Piperidine, sodium ethoxide, anhydrous ethanol, chloroform and acetonitrile were from Sinopharm Chemical Reagent (Shanghai, China). Resveratrol, Curcumin and Celastrol were from Dalin Meilun Biotecnology (Dalian, China). 3-(4,5-dimethyl-2-thiazolyl)-2,5-diphnyl-2H-tetrazolium bromide (MTT) was from Sigma-Aldrich (St. Louis, MO, USA). ^{1}H NMR and ^{13}C NMR spectrum were taken on a nuclear magnetic resonance spectrometer (Advance 400 MHz, Bruker, Switzerland). High-resolution mass spectralanalyses (HRMS) were recorded on a

High Resolution Quadrupole-time of flight mass spectrometer (Bruker, Germany). Fluorescence spectra were carried out on a fluorescence spectrometer (Edinburgh Instruments, U.K.). The fluorescence imaging was obtained with a confocal (LSM 880, Zeiss, Germany).

Synthesis of probe TCF-MQ.

Synthesis of compound 1. 3-hydroxy-3-methyl-2-butanone (1 mL, 9.5 mmol) and malononitrile (1.3 g, 20 mmol) were added into 8 mL anhydrous ethanol respectively to form a solution, then, sodium ethoxide (0.1 g, 1.5 mmol) was added, and the solution was stirred at room temperature for 1.5 h, and then refluxed at 60 °C for another 1 h. After cooling to room temperature, the precipitate was filtered to give compound 1 (1.1 g, yield: 60%). ^{1}H NMR (Chloroform-*d*, 400MHz): δ= 2.37 (s, 3H), 1.63 (s, 6H); ^{13}C NMR (Chloroform-*d*, 101MHz): δ=182.69, 175.25, 111.06, 110.44, 109.00, 104.80, 99.82, 58.44, 24.37, 14.23. HRMS: (ESI, m/z) Calcd for $C_{11}H_9N_3O$ [M−H]$^-$: 198.0661, found: 198.0694.

Synthesis of compound 2. Compound 1 (160 mg, 0.8 mmol) and 3-quinolinecarboxaldehyde(151 mg, 0.96 mmol) were dissolved in 15 mL anhydrous ethanol, two drops piperidine and acetic acid were added and the solution was refluxed for 2 h. After cooling to room temperature, the precipitate was filtered to obtain compound 2 (190 mg, yield: 70%). ^{1}H NMR (DMSO-d_6, 400MHz): δ=9.41 (d, J = 2.2 Hz, 1H), 8.97 (d, J = 2.2 Hz, 1H), 8.17–8.02 (m, 3H), 7.88 (t, J = 8.0 Hz, 1H), 7.71 (t, J = 7.5 Hz, 1H), 7.54 (d, J = 16.6 Hz, 1H), 1.86 (s, 6H); ^{13}C NMR (DMSO-d_6, 101MHz): δ=177.55, 174.96, 150.90, 148.84, 144.48, 137.41, 132.15, 129.73, 129.37, 128.15, 128.08, 127.69, 117.49, 113.10, 112.26, 111.20, 100.91, 100.07, 55.37, 25.56. HRMS: (ESI, *m/z*) Calcd for $C_{21}H_{14}N_4O$ [M+H]$^+$: 339.1240, found: 339.1208.

Synthesis of TCF-MQ. A mixture of compound 2 (60 mg. 0.18 mmol) and methyl trifluoromethanesulfonate (0.1 mL, 0.92mmol) in 5 mL trichloromethane was stirred at room temperature for 24 h under nitrogen atmosphere. Ether was added after the solvent was removed in vacuo, and then the precipitate was filtered to give TCF-MQ (68 mg, yield: 75%). ^{1}H NMR (DMSO-d_6, 400MHz): δ= 10.05 (s, 1H), 9.72 (s, 1H), 8.56-8.54 (d, J = 8.0 Hz, 1H), 8.49-8.47 (d, J = 8.0 Hz, 1H), 8.36-8.34 (q, J = 8.0 Hz, 1H), 8.13–8.09 (q, J = 8.0 Hz,1H), 8.07-8.03 (d, J = 16.0 Hz, 1H), 7.66-7.62 (d, J = 16.0 Hz, 1H), 4.67 (s, 3H), 1.87 (s, 6H); ^{13}C NMR (DMSO-d_6, 101MHz): δ=177.27, 173.43, 150.93, 146.26, 140.07, 138.57, 137.12, 131.69, 131.21, 129.19, 128.82, 120.28, 119.91, 112.86, 112.05, 110.81, 103.48, 100.05, 100.00, 56.45, 46.18, 25.50. HRMS: (ESI, m/z) Calcd for $C_{23}H_{17}F_3N_4O_4S$ [M−TfO]$^+$: 353.1396, found: 353.1385.

***In vitro* detection of NAD(P)H.** The stock solution of TCF-MQ (2×10^{-3} M) was prepared in DMSO. Stock solutions of NAD(P)H and various interferential reagents (Na^+, K^+, Ca^{2+}, Mg^{2+}, Zn^{2+}, Fe^{2+}, Fe^{3+}, glycine, lysine, serine, methionine, cysteine, homocysteine, glutathione, dithiothreitol, Vitamin C, and H_2O_2, NaClO, *t*-BuOOH, NO) were prepared in double-distilled water, but superoxide anion free radical ($O_2^{-\bullet}$) was prepared from a solution of KO_2 in DMSO. For spectral measurements, the stock solution of the TCF-MQ probe was diluted with PBS buffer to give a final concentration of 10 μM. NAD(P)H and various analytes were added to the solution of TCF-MQ (10 μM) in PBS buffer (10 mM, pH = 7.4, containing 0.5% DMSO). The fluorescence emission spectra were recorded in a range from 592–800 nm (λex = 582 nm, λem = 610 nm, slit width: 5 nm/5 nm).

Cell culture. The cell culture refered to our previous paper[39]. Briefly, HepG2 cells were cultured in DMEM (high glucose) supplemented with 10% FBS and 1% antibiotics (100 U/mL penicillin and 100 mg/mL streptomycin) at 37 °C in a humidified atmosphere of 95% air (20% O_2) and 5% CO_2. For simulating the tumor hypoxic microenvironment, HepG2 cells were cultured in a mixture containing 1% O_2, 94% N_2 and 5% CO_2 using a low oxygen incubator (Bugbox M, Ruskinn, England).

Fluorescence imaging in living cells. The fluorescence of NAD(P)H and H_2O_2 was detected by confocal microscopy. Briefly, HepG2 cells (5×10^4) were seeded on glass-bottom culture dishes (15 mm) for 24 h. Then, the cells were exposed to different concentrations of three natural antioxidants for different time under hypoxic and normoxic conditions, respectively. After treatment, the cells cultured under hypoxia and normoxia were simultaneously incubated with 10 μM (1mL) NAD(P)H probe for 20 min or 10 μM (1mL) H_2O_2 probe for 15 min in FBS-free DMEM medium at 37 °C, and then, cells were washed three times with PBS buffer and imaged immediately using a confocal microscope. TCF-MQ probe was excited at 582 nm and the fluorescence emission range was set from 600-650 nm. H_2O_2 probe was excited at 532 nm and the fluorescence emission range was set from 600-700 nm.

Tumor model preparation and fluorescence imaging. All animal experiments were performed according to the Principles of Laboratory Animal Care (People's Republic of China) and the Guidelines of the Animal Investigation Committee, and approved by the local Animal Care and Use Committee. Kunmin mice were purchased from the Qingdao Daren Fucheng Animal Co., Ltd. Hepatocellular carcinoma H22 cells (1×10^7) derived from mice were injected into the abdominal cavity of mice, the ascites were formed after 5-7 days. After three passages, the ascites were used. We selected 8-week-old mice and injected H22 cells subcutaneously into the axillary lateral of the left forelimb at a density of 1×10^7 cells/mL with 100 μL per mice. After 7 days, these mice were given different concentrations of natural antioxidants through subcutaneous injection at the tumor site for different time. After treatment, the mice were subcutaneously injected with the TCF-MQ probe and incubated for 30 min. Then, the fluorescence images were obtained using an in vivo imaging system (IVIS) with 582 nm excitation and 600-650 nm collection for NAD(P)H. In addition, the tumor volume was measured by digital calipers and calculated as: volume = 0.5 × (length×width^2)[40].

Conflicts of interest

There are no conflicts to declare.

Acknowledgements

This work was supported by National Natural Science Foundation of China (21535004, 21575081, 21775091 and 91753111), the Key Research and Development Program of Shandong Province (2018YFJH0502), the Shandong Provincial Natural Science Foundation of China (ZR2014JL055) and the key research and development plan of Yantai City (2019XDHZ098).

Notes and references

1 D. Sinha, N. Sarkar, J. Biswas, A. Bishayee, *Semin. Cancer. Biol*. **2016**, 40-41, 209-232.
2 J. Y. Wang, X. Wang, X. J. Wang, B. Z. Zheng, Y. Wang, X. Wang, B. Liang, *Eur. Rev. Med. Pharmacol. Sci*. **2018**, 22, 7492-7499.
3 Shrivastava S, Jeengar MK, Reddy VS, Reddy GB, Naidu VG, *Exp. Mol. Pathol*. **2015**, 98, 313-327.
4 D. J. Colin, E. Limagne, K. Ragot, G. Lizard, F. Ghiringhelli, É. Solary, B. Chauffert, N. Latruffe, D. Delmas, *Cell. Death. Dis*. **2014**, 5, e1533.
5 F. Song, L. Zhang, H. X. Yu, R. R. Lu, J. D. Bao, C. Tan, Z. Sun, *Food. Chem*. **2012**, 132, 43-50.
6 J. H. Kim, J. O. Lee, S. K. Lee, N. Kim, G. Y. You, J. W. Moon, J. Sha, S. J. Kim, S. H. Park, H. S. Kim, *Cell. Signal*. **2013**, 25, 805-813.
7 L. J. Yan, *J. Diabetes. Res*. **2014**, 2014, 137919.
8 E. B. Rankin, A. J. Giaccia, *Science*. **2016**, 352, 175-180.
9 N. C. Denko, *Nat. Rev. Cancer*. **2008**, 8, 705-713.
10 X. X. Xiong, X. Y. Qiu, D. X. Hu, X. Q. Chen, *Mol. Pharmacol*. **2017**, 92, 246-255.
11 X. X. Fan, H. D. Pan, Y. Li, R. J. Guo, E. L. Leung, L. Liu, *Pharmacol. Ther*. **2018**, 191, 148-161.
12 M. Inoue, R. Nakashima, M. Enomoto, Y. Koike, X. Zhao, K. Yip, S. H. Huang, J. N. Waldron, M. Ikura, F. F. Liu, S. V. Bratman, *Nat. Commun*. **2018**, 9, 5116.
13 B. Petrova, K. Liu, C. Tian, M. Kitaoka, E. Freinkman, J. Yang, T. L. Orr-Weaver, *Proc. Natl. Acad. Sci. U S A*. **2018**, 115, E7978-E7986.
14 N. S. Rajasekaran, P. Connell, E. S. Christians, L. J. Yan, R. P. Taylor, A. Orosz, X. Q. Zhang, T. J. Stevenson, R. M. Peshock, J. A. Leopold, W. H. Barry, J. Loscalzo, S. J. Odelberg, I. J. Benjamin, *Cell*. **2007**, 130, 427-439.
15 H. Zhang, P. Limphong, J. Pieper, Q. Liu, C. K. Rodesch, E. Christians, I. J. Benjamin, *FASEB J*. **2012**, 26, 1442-1451.
16 D. E. Handy, J. Loscalzo, *Free. Radic. Biol. Med*. 2017, 109, 114-124.
17 S. Dimmeler, A. M. Zeiher, *Cell*. **2007**, 130, 401-402.
18 A. C. Brewer, S. B. Mustafi, T. V. Murray, N. S. Rajasekaran, I. J. Benjamin, *Antioxid. Redox. Signal.* **2013**, 18, 1114-1127.
19 H. Komatsu, Y. Shindo, K. Oka, J. P. Hill, K. Ariga, *Angew. Chem. Int. Ed. Engl*. **2014**, 53, 3993-3995.
20 V. A. Aleshin, A. V. Artiukhov, H. Oppermann, A. V. Kazantsev, N. V. Lukashev, V. I. Bunik, *Cells*. **2015**, 4, 427-451.
21 L. Yuan, W. Y. Lin, K. B. Zheng, L. W. He, W. M. Huang, *Chem. Soc. Rev*. **2013**, 42, 622–661.
22 J. Yin, Y. Kwon, D. Kim, D. Lee, G. Kim, Y. Hu, J. H. Ryu, J. J. Yoon, *Am. Chem. Soc*. **2014**, 136, 5351-5358.
23 X. Ao, S. A. Bright, N. C. Taylor, R. B. P Elmes, *Org. Biomol. Chem*. **2017**, 15, 6104-6108.
24 A. Tirla, P. Rivera-Fuentes, *Angew. Chem. Int. Ed. Engl*. **2016**, 55, 14709-14712.
25 A. Tirla, P. Rivera-Fuentes, *Chimia (Aarau)*. **2018**, 72, 241-244.
26 C. A. Roeschlaub, N. L. Maidwell, M. R. Rezai, P. G. Sammes, *Chem. Commun.* **1999**, 1637-1638.
27 C. Tu, R. Nagao, A. Y. Louie, *Angew. Chem. Int. Ed*. **2009**, 48, 6547-6551.
28 S. O. Jung, J. Y. Ahn, S. Kim, *Tetrahedron. Letters*. **2010**, 51, 3775-3778.
29 H. Komatsu, Y. Shindo, K. Oka, I. P. Hill, K. Ariga, *Angew. Chem. Int. Ed*. **2014**, 53, 3993-3995.
30 M. A. Fomin, R. I. Dmitrev, J. Jenkins, D. B. Papkovsky, D. Heindl, B. Konig, *ACS. Sens*. **2016**, 1, 702-709.
31 L. Wang, J. Zhang, B. Kim, J. Peng, S. N. Berry, Y. Ni, D. Su, J. Lee, L. Yuan, Y. T. Chang, *J. Am. Chem. Soc.* **2016**, 138, 10394-10397.
32 Y. Zhao, K. Wei, F Kong, X. Gao, K. Xu, B. Tang, *Anal. Chem*. 2018, 91, 1368-1374.
33 C. Zhang, L. R. Dalton, M-C. Oh, H. Zhang, W. H. Steier, *Chem. Mater*. **2001**, 13, 3043-3050.
34 W. Bentoumi, J. C. Mulatier, P. A. Bouit, O. Maury, A. Barsella, J. P. Vola, E. Chastaing, L. Divay, F. Soyer, P. Le Barny, Y. Bretonnière, C. Andraud, *Chemistry*. **2014**, 20, 8909-8913.
35 A. C. Sedgwick, H. H. Han, J. E. Gardiner, S. D. Bull, X. P. He, T. D. James, *Chem. Commun (Camb)*. **2017**, 53, 12822-12825.
36 L. B. Jiang, L. Cao, Y. Q. Ma, Q. Chen, Y. Liang, F. L. Yuan, X. L. Li, J. Dong, N. Chen, *Osteoarthritis. Cartilage*. **2018**, 26, 138-148.
37 O. Polesskaya, A. Sun, G. Salahura, J. N. Silva, S. Dewhurst, K. Kasischke, *J. Vis. Exp*. 2012, pii: 3466.
38 X. Liu, B. Hu, R. Cheng, F. Kong, X. Pan, K. Xu, B. Tang, *Chem. Commun (Camb)*. 2016, 52, 6693-6696.
39 X. H. Pan, X. X. Song, C. Wang, T. T. Cheng, D. R. Luan, K. H. Xu, B. Tang, *Theranostics*. **2019**, 9, 1794-1808.
40 W. S. Henry, T. Laszewski, T. Tsang, F. Beca, A. H. Beck, S. S. McAllister, A. Toker, *Cancer. Res*. **2017**, 77, 790-801.

View Article Online
DOI: 10.1039/C9SC02020A

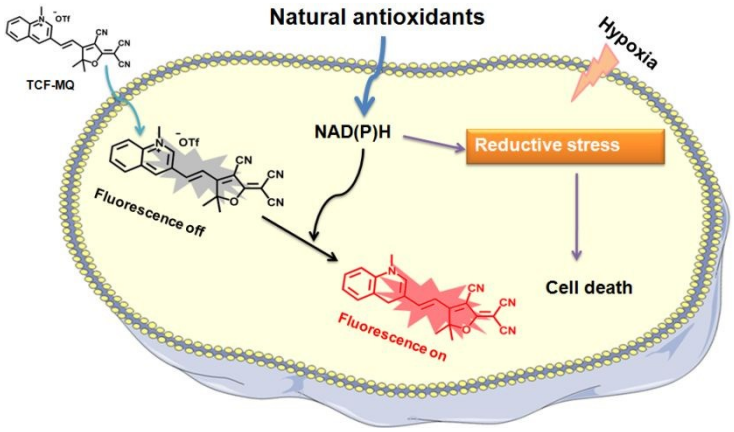

An ultrasensitive fluorescent probe for monitoring NAD(P)H and revealing reductive stress induced by natural antioxidants in HepG2 cells under hypoxia.